Current Mode Controlled LCC Resonant Converter for Electrical Discharge Machining Applications

Rosario Casanueva, Manuel Ochoa, Francisco J. Azcondo, Salvador Bracho
University of Cantabria
Dept. of Electronics Technology, Systems and Automation Engineering
Av. de los Castros, s/n. 39005 Santander, Spain
{charo, ochoa, azcondo, bracho}@teisa.unican.es

Abstract — **In this paper, a contribution to the Electrical Discharge Machining (EDM) technology is presented. The final aim of this research is to develop small size EDM systems and determine the influence of the voltage and current of the output electrical arc on the quality and efficiency of the workpiece machining. The proposed system is a dc to dc LCC resonant converter intended to generate current controlled arc pulses at a constant frequency that erode the workpiece.**

The benefits of this proposal are the following: 1) the system has inherent protection under short circuit, 2) a simple linear controller results in a highly robust feedback control under load changes and 3) the transistors turn-on at zero voltage is guaranteed at any load value. The output voltage is intended to be adjusted by an external system that controls the arc distance.

I. INTRODUCTION

Electrical Discharge Machining (EDM) is an electrothermal process. EDM uses an electrode positioned at a fixed small distance (spark gap) above the workpiece, both submerged in a dielectric fluid. A pulsating dc power supply or EDM generator applies voltage pulses between the electrode and workpiece generating sparks or current conduction through the gap. Each spark results in localized heating that melts a small area of the workpiece surface. (Fig. 1).

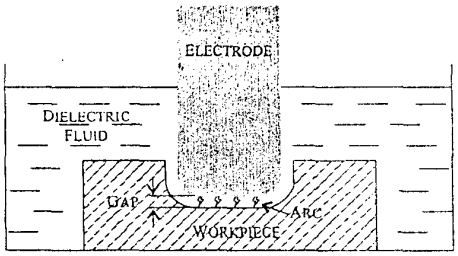

Fig. 1. Basic EDM process.

Basically, an EDM system consists of the following main components [1]:

- Workpiece and electrode.
- Dielectric fluid.
- DC power supply.
- Servomechanism, to maintain a constant gap.

The metal removal rate (MRR) and the surface finish depend on the magnitude and duration of the discharge. As the current is increased, so does the MMR but the surface finish decreases. As the discharge frequency is increased, the surface finish improves but the electrode wear increases [1], [2].

There are two types of EDM power supplies:

a) Isoenergetic, which provides constant energy pulses, achieving good finishes, its drawback is that if the off-time is very long, the electrode wear increases, and as the frequency decreases, the MRR diminishes.
b) Isofrequencial, which keeps the discharge frequency constant, ensuring the MRR.

This work presents the design of the dc to ac stage of an isofrequencial EDM power supply implemented with a current source, full bridge LCC resonant inverter to take advantage of its performance with regard to the controllability, efficiency, size and really cost-effectiveness.

The main application of this work is the field machining to provide maintenance and reparation services to nuclear or traditional power plants or any industrial plant. EDM is an adequate technique to perform machining tasks in nuclear plants because it does not produce chips that could cause damage to reactor components. In EDM, micron size particles are immediately flushed away with the dielectric fluid. In addition, it is ideally suited for underwater applications.

II. PROPOSED EDM SUPPLY

The EDM generator must provide the voltage and current waveforms [3] as depicted in Fig. 2.

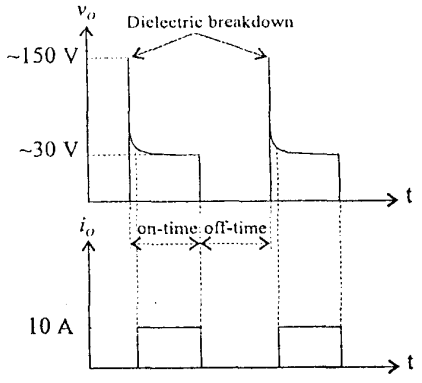

Fig. 2. Specified EDM waveforms.

The machining frequency is specified to be up to 10 kHz. During the on-time the generator applies the potential difference between the electrode and workpiece to generate and sustain the current through the arc, and during the off-time the output power is interrupted, causing the arc current drop down to zero. The generator must increase the voltage between the electrode and the workpiece up to 150 V to ionize the dielectric, that is modeled as

an output resistance with a value close to an open circuit condition.

Once the dielectric resistance is overcome the generator must sustain an operating point where the arc voltage is around 28 V and the current is regulated around 10 A until the end of the on-time.

The proposed solution for the EDM requirements is a full-bridge LCC resonant converter operating at a switching frequency of 200 kHz, used as a current source and is shown in Fig. 3. The design sequence of the LCC resonant inverter is oriented to achieve the dielectric breakdown and current stabilization with maximum stress on the components limited by design. The converter topology is such that, working above the resonant frequency, the transistors turn on at zero voltage, resulting in minimum switching losses.

The full bridge configuration has been chosen because of its capability of converting high power. As the continuous change in the gap distance may lead to load changes from open to short circuit conditions, the resonant inverter is designed as a current source to provide the system with inherent protection under short circuit conditions. The open circuit fault must be limited by an over-voltage protection.

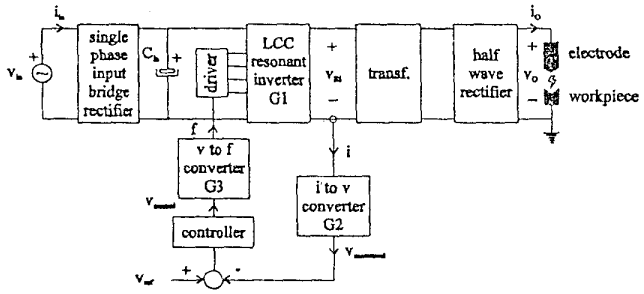

Fig. 3. Basic block diagram of the current controlled EDM system using a LCC resonant inverter.

III. CURRENT SOURCE, LCC RESONANT INVERTER DESIGN

Fig. 4 (a) shows the full bridge LCC resonant inverter. The circuit input is the utility line rectified voltage, the full bridge topology applies a square-wave voltage, v_{AB}, to the resonant network. The waveforms in the resonant circuit are sine waves, so essentially a sine wave appears at v_{AB}. This analysis method is called the fundamental approximation [4], the first harmonic of v_{AB} is applied to the resonant circuit as shown in Fig. 4 (b).

This circuit is described by the following parameters:

- The ratio of the capacitances,

$$A = \frac{C_p}{C_s} \tag{1}$$

- the parallel resonant frequency,

$$\omega_p = \frac{1}{\sqrt{LC_p}} \tag{2}$$

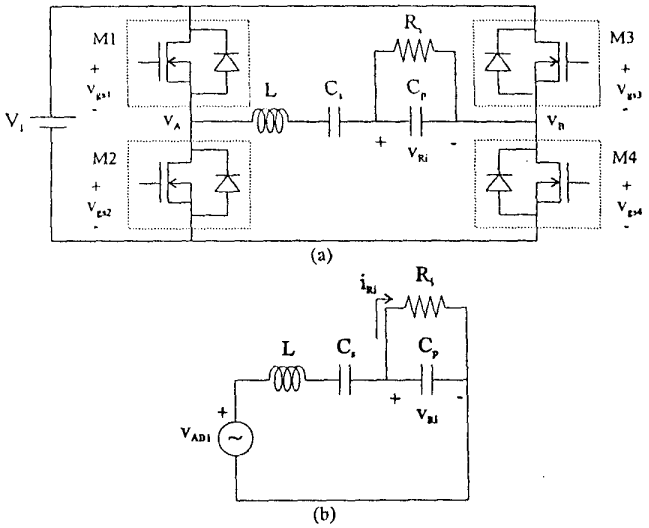

Fig. 4. (a) Full bridge LCC resonant inverter.
(b) Simplified circuit.

- the characteristic impedance at ω_p,

$$Z_p = \omega_p L = \frac{1}{\omega_p C_p} \tag{3}$$

- the parallel quality factor,

$$Q_p = \frac{R_i}{Z_p} \tag{4}$$

To design the LCC resonant inverter as a current source, the peak current through the equivalent resistance expression [5] is analyzed,

$$\hat{I}_{Ri} = \frac{4V_I}{\pi Z_p Q_p} \sqrt{\frac{1+Q_p^2\left(\frac{\omega}{\omega_p}\right)^2}{1+\left[\frac{1}{Q_p}\left(\frac{\omega}{\omega_p}-\frac{\omega_p}{\omega}A\right)\left(1+Q_p^2\left(\frac{\omega}{\omega_p}\right)^2\right)-Q_p\frac{\omega}{\omega_p}\right]^2}} \tag{5}$$

Expression (5) has no dependence on the load at the frequency,

$$\omega = \omega_p\sqrt{A+1} = \omega_0 \tag{6}$$

where ω_0 is the unloaded natural resonant frequency of the LCC circuit.

Thus, at this frequency, the equivalent resistance peak current becomes,

$$\hat{I}_{Ri}\Big|_{\omega=\omega_0} = \frac{4V_I}{\pi Z_p}\sqrt{A+1} \tag{7}$$

for any value of R_i.

From (3), (6) and (7) the parallel capacitance is obtained for a given $\hat{I}_{Ri}$.

$$C_p = \frac{\hat{I}_{Ri}\big|_{\omega=\omega_0}}{8V_I f_0} \tag{8}$$

Taking into account the inverter parameters (1) and (3), the expressions of the series capacitance and the inductor are given by,

$$C_s = \frac{C_p}{A} = \frac{\hat{I}_{Ri}\big|_{\omega=\omega_0}}{8AV_I f_0} \tag{9}$$

$$L = \frac{2(A+1)V_I}{\pi^2 f_0 \hat{I}_{Ri}\big|_{\omega=\omega_0}} \tag{10}$$

These expressions depend on the input voltage, V_I, the resonant frequency, f_0, and the required equivalent resistance peak current, $\hat{I}_{Ri}$.

The transformer turns ratio, n, is calculated by

$$n = \frac{\hat{V}_{Ri,max}}{\hat{V}_{O,max}} = \frac{2\hat{V}_{Ri,max}}{\pi V_{O,max}} \tag{11}$$

where $V_{O,max}$ is the specified maximum value of the average output voltage and $\hat{V}_{Ri,max}$ is the maximum value of the peak current through R_i.

Thus, the equivalent resistance peak voltage is obtained by,

$$\hat{V}_{Ri} = \frac{\pi n V_O}{2} \tag{12}$$

where V_O is the average value of the on-state output voltage.

As a first approach the half wave rectifier is considered with no conduction losses, so the equivalent resistance, that models the rectifier and the load, and the current through it are finally obtained by,

$$R_i = \frac{\hat{V}_{Ri}^2}{2P_O} \tag{13}$$

$$\hat{I}_{Ri} = \frac{\hat{V}_{Ri}}{R_i} \tag{14}$$

The following steps summarize the design sequence:

- The input data: V_I, $\hat{V}_{Ri,max}$, V_O, $V_{O,max}$, P_O, f, are collected.
- Using (11), the transformer turns ratio, n, is obtained.
- From (12) and (13) peak equivalent resistance voltage and R_i, are calculated.
- Substitution of the resulting values of $\hat{V}_{Ri}$ and R_i into (14) yields the equivalent resistance current, $\hat{I}_{Ri}$.
- From (8), C_p is obtained, the closer standard value is chosen and the frequency, f, is re-calculated.
- Finally, a value of A is selected and using (9) and (10) the values of C_s and L are obtained.

IV. CONTROLLER DESIGN

A controller has been developed to establish the switching frequency of the resonant inverter around ω_0 to fix the desired output current during the on-time and above ω_0 during the off-time. It should be noted that the behaviour of the LCC inverter is highly dependent on the load except if, for current source operation, the switching frequency is ω_0 and at this frequency the inverter is designed to deliver the nominal output current. In this case, the design of a simple linear feedback control results in a highly robust control.

Firstly, the Bode diagram of the system that represents the transfer functions of the output current versus the switching frequency of the LCC resonant inverter, the voltage to frequency converter and the current to voltage converter that provides the feedback is found. To achieve this, a small signal equivalent circuit of them is obtained to be simulated with PSpice and find its frequency response.

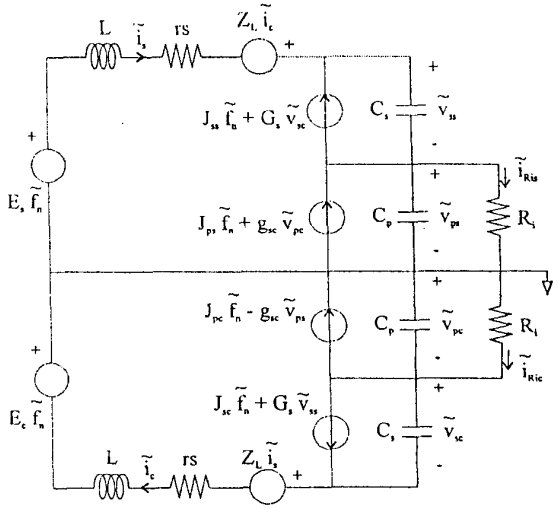

$f_n = f/f_0$

$E_c = -I_s\,\omega_0 L$

$E_s = I_c\,\omega_0 L$

$Z_L = \Omega L$

$J_{ss} = V_{sc}\,\omega_0 C_s$

$J_{sc} = V_{ss}\,\omega_0 C_s$

$G_s = \Omega C_s$

$g_{sc} = \Omega C_p$

$J_{ps} = V_{pc}\,\omega_0 C_p$

$J_{pc} = -V_{ps}\,\omega_0 C_p$

$$K_s' = \frac{2}{\pi N_s R_i}\frac{V_{ps}}{(V_{pc}^2+V_{ps}^2)^{1/2}}$$

$$K_c' = \frac{2}{\pi N_s R_i}\frac{V_{pc}}{(V_{pc}^2+V_{ps}^2)^{1/2}}$$

Fig. 5. Small signal equivalent circuit model of the LCC resonant inverter and the current to voltage converter.

The small signal model used is developed in [6] for dc/dc LCC resonant converters. It is modified to adapt it to the study of the inverter stage (G1 in Fig. 3) in addition to the current to voltage converter that provides the feedback signal (G2 in Fig. 3). The latter is used to measure the current and it basically consists of a current transformer, a rectifier and a load to convert current into voltage [7]. The resulting small signal equivalent circuit is shown in Fig. 5.

The voltage to frequency converter gain (G3 in Fig. 3) is found experimentally and it is included to perform the simulation to plot the Bode diagram. Using straight-line approximation on the simulated Bode plot, a second-order transfer function is obtained and its Bode diagram (G1*G2*G3) is shown in Fig. 6.

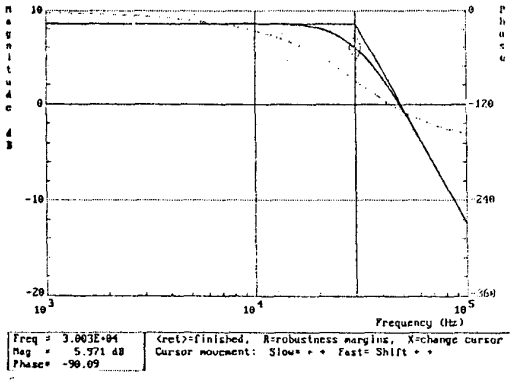

Fig. 6. Bode diagram of the small signal equivalent circuit.

The specifications established for the whole system are a phase margin, PM = 60° at a crossover frequency fc = ωc/2π = 30 kHz, well above the switching frequency.

The proposed controller is a Type 2 controller according to the following transfer function [8],

$$Gc(s) = \frac{A\,(s + \omega z)}{s\,(s + \omega p)}$$

The Bode diagram and circuit topology are shown in Fig. 7.

The design of the controller results in the following values R_1 = 1.72 kΩ, R_2 = 560 Ω, C_1 = 57 nF and C_2 = 1.8 nF, and the Bode diagram is shown in Fig. 8 (a). Fig. 8 (b) shows the Bode diagram for the open-loop system, which fits the specified requirements of phase margin and crossover frequency.

V. EXPERIMENTAL RESULTS

At present, different prototypes have been designed based on the techniques presented in this paper. These preliminary results confirm a stable behaviour under the control criteria of the inverter working at high frequency in the constant current operating point in contrast with other design techniques based on the reduction of the reactive power in the LCC converter. In this section these preliminary results are presented.

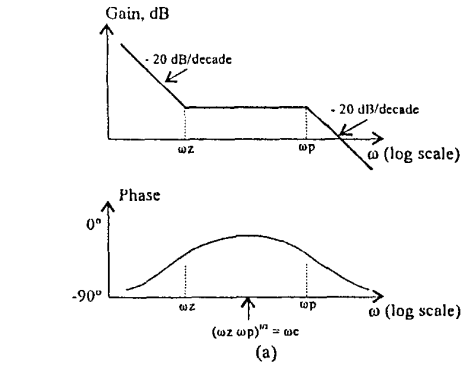

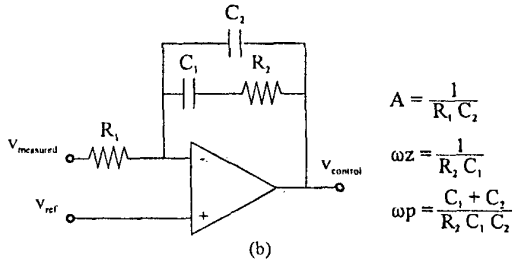

Fig. 7. Type 2 controller: (a) Bode diagram. (b) Circuit implementation

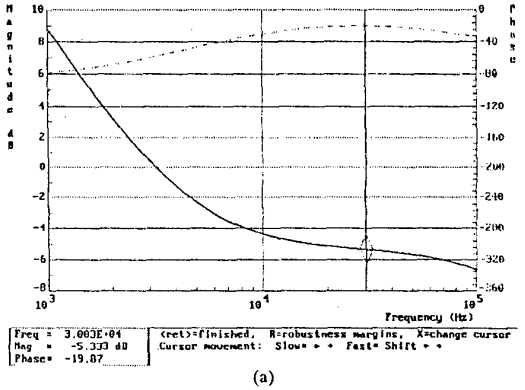

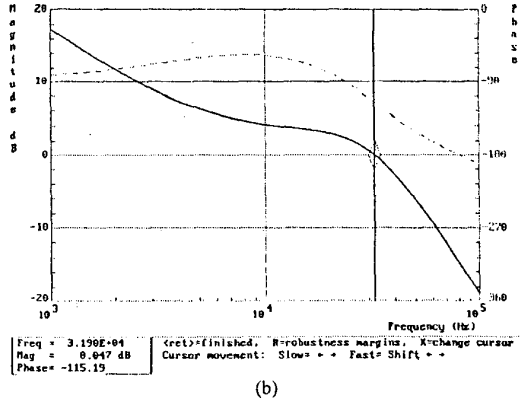

Fig. 8. Bode diagrams: (a) of the controller, (b) of the open-loop system.

The resonant inverter is designed following the design sequence proposed in Section III with V_I = 280 V, $\hat{V}_{Ri,max}$ = 2500 V, V_O = 28 V, $V_{O,max}$, =150 V, P_O = 500 W, f = 200 kHz. The resulting circuit parameters are shown in Table 1. The actual value of the constructed inductance, L, is ~160 μH and the load resistance, R_i, is 249 Ω. The switching frequency is chosen to be 208 kHz, just above the resonant frequency, f_0, to assure continuous conduction mode under all load conditions. The MOSFET transistor selected was the IRFP450 and the circuit IR2111 as driver.

The circuit has been verified by emulating the gap resistance by means of R_i connected to C_p.

TABLE I
CIRCUIT IMPLEMENTATION MAIN PARAMETERS

n	$\hat{V}_{Ri}$ (V)	R_i (Ω)	$\hat{I}_{Ri}$ (A)	C_p (nF)	f (kHz)	A	C_s (nF)	L (μH)
10	500	250	2	4.7	205	0.25	20	157

Fig. 9 shows the transistors switching current and voltage at turn on transition, the reference voltage, v_{ref}, changes from 0 V to 2.8 V at 10 kHz. During the off-time the switching frequency is 333 kHz and during the on-time is 208 kHz.

Fig. 10 shows the experimental waveform of the output current of the inverter for a reference voltage, v_{ref}, that changes from nominal operation to arc extinction and vice versa at 10 kHz. During the on-time, v_{ref} = 2.8 V, the system provides a stabilized value of current amplitude equal to 2 A and during the off-time, v_{ref} = 0 V, the current amplitude is 0.6 A. It is expected that in the second case the rectified output current drops below the arc hold current, causing the arc extinction.

Fig. 11 shows the inverter output voltage, the value of the voltage amplitude is 508 V and the power delivered to the full load is 516 W.

Even in the case of being far away of the desired gap distance which may produce a load deviation from the nominal value, the power supply provides the specified current as shown in Fig. 12 where a load change has been emulated using 500 Ω (150% of full load) connected to C_p. During the on-time the current amplitude is 1.8 A and during the off-time the current amplitude is 0.32 A.

Fig. 13 shows the output current under short circuit conditions. The output current is within the operation range if the electrode and the workpiece would contact somehow.

As it has been mentioned above the gap resistance is emulated by means of fixed values of resistance, R_i. To verify the inverter performance under all load conditions a discharge lamp type Sylvania SHP 250W has been connected to the circuit. The high-pressure sodium (HPS) lamp behaves like a resistance that changes from open circuit, in the off-state, to short circuit, just after ignition. The results of this experiment are shown in Fig. 14. Fig. 14 (a) shows the output voltage transient, the ignition voltage amplitude reaches 1.65 kV and then drops to the short circuit condition. Fig. 14 (b) shows the output current transient, when the lamp ignition is achieved a short circuit current flows through the lamp.

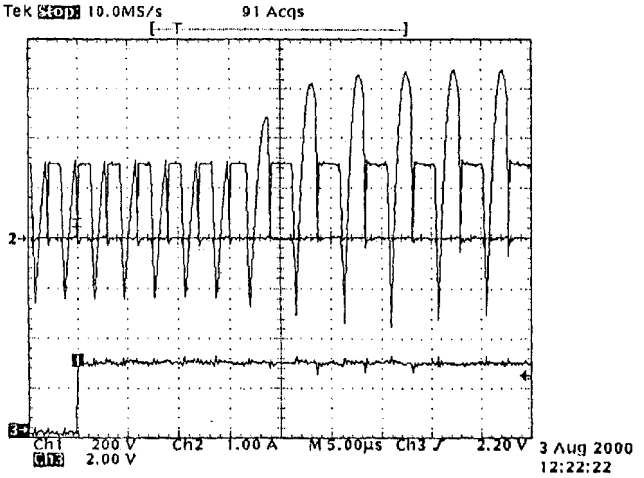

Fig. 9. Switching current and voltage at turn on transition.

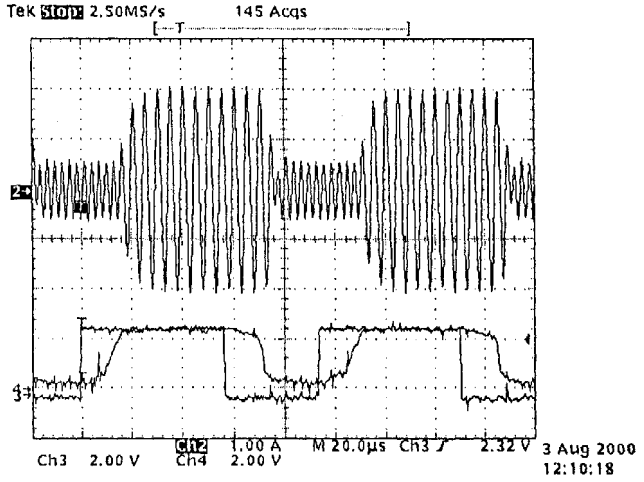

Fig. 10. Output current waveform. Full load.

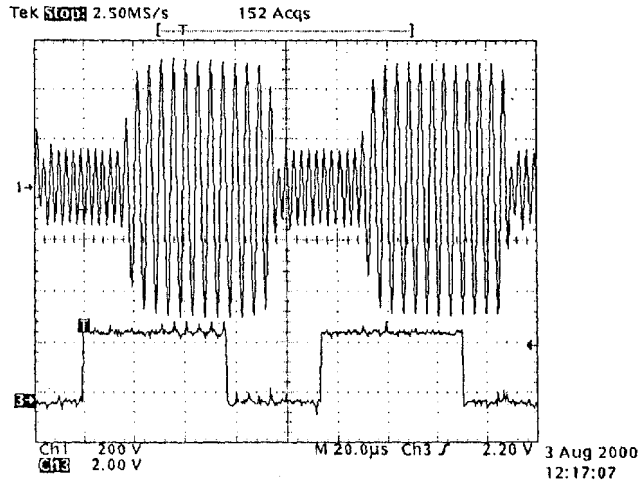

Fig. 11. Output voltage waveform. Full load.

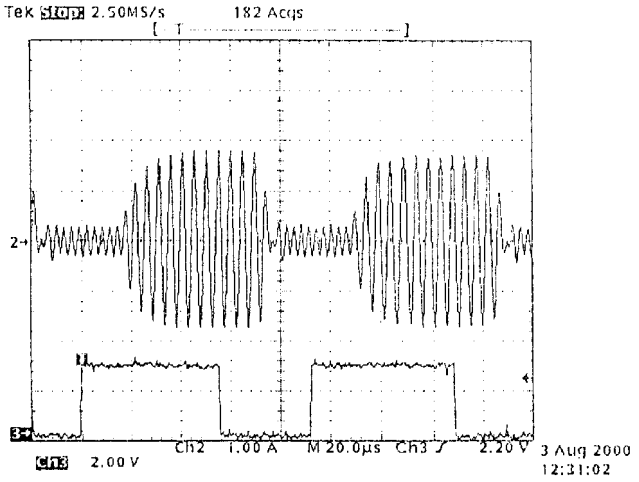

Fig. 12. Output current waveform. 150% of full load.

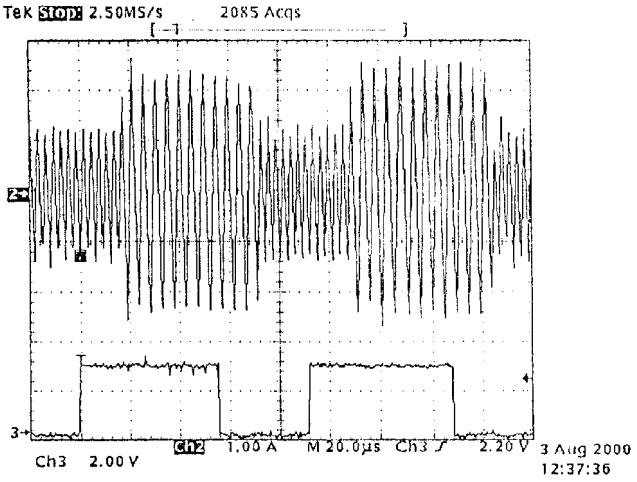

Fig. 13. Output current under short circuit condition.

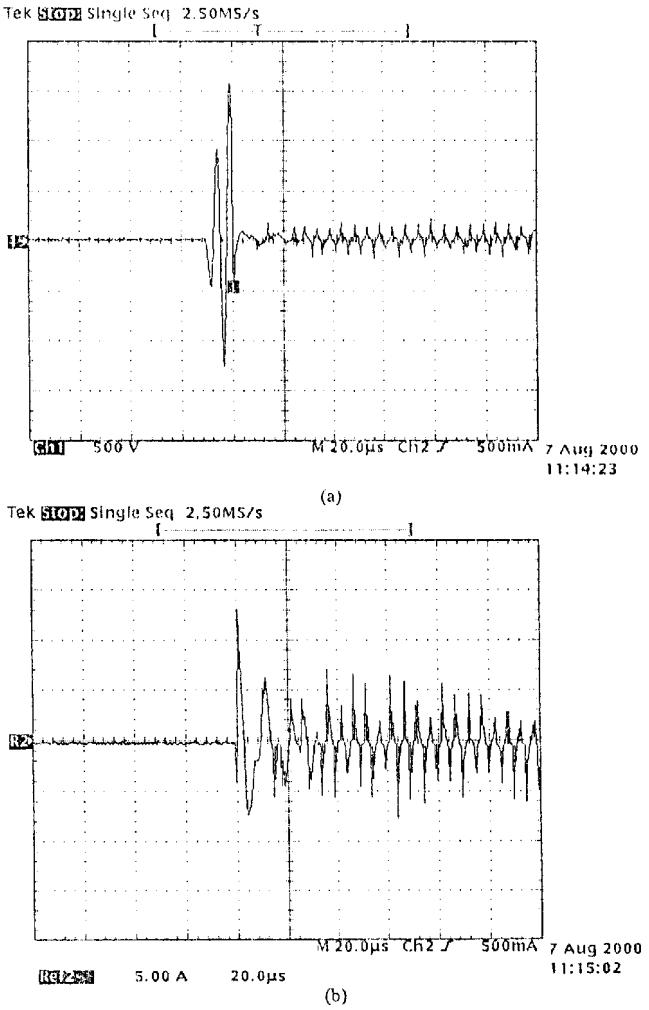

Fig. 14. Output waveforms from open circuit to short circuit. (a) Voltage. (b) Current. Load: HPS Lamp.

VI. CONCLUSIONS

A resonant converter topology such as the LCC converter has been proved to be well suited to fulfill the EDM requirements with the addition of further performances regarding efficiency and current stability under very irregular load conditions. The design strategy imposes a nominal operating point where the converter behaves as a current source then a feedback loop corrects the deviations over the nominal current value, achieving very good current stability performance under load changes with a simple linear control. Up to now different experiments have been carried out on a prototype of the LCC inverter stage, emulating the arc between the electrode and the workpiece by its equivalent resistance. The dimensions of the first prototype is around ten times smaller than the present system in operation. Further works are in progress to develop the transformer, rectifier and over-voltage protection to verify the whole system performance.

REFERENCES

[1] G. Boothroyd, W. A. Knight, *Fundamentals of Machining and Machine Tools*. 2nd Edition. New York: Marcel Dekker, 1989.

[2] E. Bud Guitrau, *The EDM Handbook*. Hanser Gardner Publications, 1997.

[3] Electrical Discharge Machining; concepts, methods, application. Standard VDI 3400. June 1975.

[4] R. L. Steigerwald. "A Comparison of Half-Bridge Resonant Converter Topologies", *IEEE Transactions on Power Electronics*, Vol. 3, No. 2, pp. 174-182, April 1988.

[5] Marian K. Kazimierzuk, Dariusz Czarkowski, *Resonant Power Converters*. New York: Wiley Interscience Publication, 1995.

[6] E. X. Yang, F. C. Lee, and M. M. Jovanóvic. "Small-signal modeling of LCC Resonant Converter", *IEEE PESC*, 1992.

[7] C. W. T. McLyman, *Transformer and Inductor Design Handbook*. 2nd Ed. New York: Marcel Dekker, 1988.

[8] Abraham I. Pressman, *Switching Power Supply Design*. New York: McGraw-Hill, Inc. 1991.

[9] N. Mohan, T. M. Underland, W. P. Robbins, *Power Electronics: Converters Applications and Design*. 2nd Edition. New York: Wiley and Sons, 1995.